bioRxiv preprint doi: https://doi.org/10.1101/2021.06.04.447066; this version posted June 4, 2021. The copyright holder for this preprint (which was not certified by peer review) is the author/funder. All rights reserved. No reuse allowed without permission.

Human single-chain antibodies neutralize SARS-CoV-2 variants by engaging an essential epitope of the spike: a new weapon against COVID-19

Olga Minenkova[1], Daniela Santapaola[1], Ferdinando Maria Milazzo[1], Anna Maria Anastasi[1], Gianfranco Battistuzzi[1], Caterina Chiapparino[1], Antonio Rosi[1], Giuseppe Gritti[2], Gianmaria Borleri[2], Alessandro Rambaldi[2,3], Clélia Dental[4], Cécile Viollet[4], Bruno Pagano[5], Laura Salvini[6], Emanuele Marra[7], Laura Luberto[7], Antonio Rossi[8], Anna Riccio[9], Emilio Merlo Pich[1], Maria Gabriella Santoro[8,9] and Rita De Santis[1*]

[1]Alfasigma SpA, Biotechnology R&D, Pomezia, Rome, Italy; [2]Papa Giovanni XXIII Hospital, Bergamo, Italy; [3]Department of Hematology and Oncology, University of Milan, Italy; [4]Texcell EVRY Cedex, France; [5]Department of Pharmacy, University of Naples Federico II; [6]Toscana Life Sciences; [7]Takis Biotech, Rome, Italy; [8]Institute of Translational Pharmacology, CNR, Rome, Italy; [9]Department of Biology, University of Rome Tor Vergata, Rome, Italy

*Corresponding author

Rita De Santis PhD rita.desantis@alfasigma.com https://orcid.org/0000-0002-5037-0611

Alfasigma SpA, Biotechnology R&D Via Pontina Km 30.400 Pomezia 00071, Rome, Italy

Keywords: Coronavirus; SARS-CoV-2; single chain Fv antibody; viral variants

bioRxiv preprint doi: https://doi.org/10.1101/2021.06.04.447066; this version posted June 4, 2021. The copyright holder for this preprint (which was not certified by peer review) is the author/funder. All rights reserved. No reuse allowed without permission.

Abstract

As of June 2021, severe acute respiratory syndrome coronavirus 2 (SARS-CoV-2) remains a global emergency and effective therapeutic interventions for the treatment and prevention of coronavirus disease 2019 (COVID-19) are urgently needed. SARS-CoV-2-neutralizing monoclonal antibodies (mAbs) represent a promising approach to COVID-19 therapy. However, the recently described accumulating mutations in the SARS-CoV-2 spike protein are challenging the efficacy of approved and investigational mAbs, whose widespread use is also hampered by their significant costs and possible side effects, including Antibody-Dependent Enhancement (ADE). Here we describe a cluster of SARS-CoV-2 neutralizing human single chain variable fragment antibodies, identified by phage display, sharing a common VH CDR3 sequence. Phage libraries were built by amplifying variable domains of immunoglobulin genes from cDNA derived from lymphocytes of COVID-19 convalescent subjects living in Bergamo, Italy. The scFv76-cluster antibodies (scFv76-cl Abs) exhibit high affinity for the spike receptor binding domain (RBD) of Wuhan strain and emerging variants, leading to inhibition of RBD/human ACE2 interaction. The antigenic epitope recognized by scFv76 was mapped in the receptor binding motif (RBM) of RBD at residues L455, F456, Y473, N487 and Y489. None of these residues has been to date listed among the RBD mutations of SARS-CoV-2 variants of concern (VOCs), suggesting an important role of such epitope in viral infectivity. Treatment with scFv76-cl Abs is effective against SARS-CoV-2, as determined by *in vitro* experiments of viral infection, replication, cytopathogenicity and spike-mediated syncytia formation. Moreover, their intranasal administration is shown to counteract infection in two independent animal models. Overall, the biochemical and biological characteristics of scFv76-cl Abs are compatible with their clinical use for COVID-19 therapy by intranasal or aerosol administration. To our knowledge, this is the first example of promising human anti-SARS-CoV-2 scFv antibodies as drug candidates for COVID-19 therapy.

bioRxiv preprint doi: https://doi.org/10.1101/2021.06.04.447066; this version posted June 4, 2021. The copyright holder for this preprint (which was not certified by peer review) is the author/funder. All rights reserved. No reuse allowed without permission.

Introduction

After more than one-year since the SARS-CoV-2 pandemic began, just a few lifesaving drugs have been approved for COVID-19 treatment and the medical community is urgently calling for both massive vaccination and novel therapies. Specific monoclonal antibodies (mAbs) able to bind to the 'spike' protein and neutralize SARS-CoV-2 in infected patients represent a potential strategy for antiviral intervention. To date, several neutralizing mAbs have been developed, some of which are now approved or under the evaluation of regulatory authorities (*1*). Nevertheless, traditional mAbs are not devoid of hurdles. First, they are at risk of inducing Antibody Dependent Enhancement (ADE) of infectious diseases as described with mAbs employed in several viral infections, including SARS-CoV-2 (*2*). Second, they are very expensive, being produced in mammalian expression systems and requiring high dose administered by parenteral infusion performed in hospital settings. Third, the recommended use has been restricted to subjects at the very early stage of COVID-19, in practice to those at risk of progressing into life-threatening severe COVID-19, since they proved to be ineffective when dosed at later stages (*3*).

An interesting alternative is offered by antibodies in the format of single-chain variable fragments (scFv) generated by engineering in a single polypeptide both variable heavy and light chain sequences of immunoglobulins, joined via a flexible peptide linker that allows reconstitution of functional antigen binding domains (**Figure 1a top panel)** (*4*). The first human scFv antibody approved by the U.S. Food and Drug Administration (FDA) on October 2019 for topical use is Brolucizumab, a vascular endothelial growth factor (VEGF) blocker, for the treatment of exudative age-related macular degeneration (*5*).

ScFv molecules offer several theoretical advantages over traditional mAbs. In fact, they are devoid of the immunoglobulin Fc exerting immune effector function, and therefore are not at risk of inducing ADE. In addition, they are less costly than mAbs due to their rapid production at large scale in non-mammalian expression systems. Because of the small size (27 kDa versus 150 kDa of mAbs) and low complexity (no glycosylation, simpler structure), scFv antibodies are expected to be

bioRxiv preprint doi: https://doi.org/10.1101/2021.06.04.447066; this version posted June 4, 2021. The copyright holder for this preprint (which was not certified by peer review) is the author/funder. All rights reserved. No reuse allowed without permission.

particularly stable and suitable for topical use, i.e. by intranasal drops/spray or aerosol nebulization, therefore allowing dosing in non-hospital settings. Because of such advantages, the possible use of scFv antibodies in the SARS-CoV-2 pandemic is gaining interest and consequently we decided to pursue the human scFv antibody format for prevention and treatment of SARS-CoV-2 infection by topical use.

We isolated human scFv antibodies from phage display libraries built by amplifying immunoglobulin genes from cDNA derived from lymphocytes of COVID-19 convalescent donors from Bergamo, Italy. This approach aimed at maximizing the possibility to select affinity-matured antibody species against the 'spike', a trimeric class I fusion protein anchored into the viral envelope and essential for SARS-CoV-2 entry into the cells (*6,7*).

As most viral fusion proteins, each monomer of the spike is synthesized as a fusogenically-inactive precursor, which assembles into an inactive homotrimer and is endoproteolytically cleaved by cellular proteases, giving rise to a metastable complex of two functional subunits: the N-terminal subunit (S1) which contains the receptor binding domain (RBD) and a C-terminal subunit (S2) which contains the fusion peptide. The RBD domain spans from residue 333-527 and binds to the extracellular domain of human angiotensin-converting enzyme 2 (ACE2).

Within the spike RBD a receptor binding motif (RBM) was identified, spanning from residue 438 to 506, that resulted essential for ACE2 binding (*8*). Via the RBD the spike of SARS-CoV-2 binds more tightly to ACE2 than the homologous SARS-CoV-1 accounting for higher transmissibility of SARS-CoV-2.

Selection of scFv candidates was performed applying highly stressing conditions during panning of scFv phage display libraries over the RBD of SARS-CoV-2 spike protein. This procedure allowed the selection of six highly homologous antibodies, overall named scFv76-cluster, sharing a novel VH CD3 sequence and exhibiting high affinity for an epitope of the RBM of the spike RBD. Herein we present findings from *in vitro* and *in vivo* experiments that support further development of scFv76-cl Abs as a new therapeutic tool for topical use in SARS-CoV-2 infections.

bioRxiv preprint doi: https://doi.org/10.1101/2021.06.04.447066; this version posted June 4, 2021. The copyright holder for this preprint (which was not certified by peer review) is the author/funder. All rights reserved. No reuse allowed without permission.

Results

Selection of human scFv antibodies against SARS-CoV-2 spike RBD

A schematic representation of mAbs compared to scFv format and the flow chart of the project steps are given in **Figure 1a**. With the aim to select the source of most matured anti-SARS-CoV-2 antibody sequences, we investigated the antibody response of ten convalescent COVID-19 subjects. Serum samples, collected after double negative swab, were analyzed for binding to the spike protein, inhibition of spike/ACE2 interaction and viral neutralization. As shown in **Figure 1b (top panel)**, six out of ten COVID-19 sera (CS) were found to strongly bind to the viral spike (Wuhan strain), while four exhibited lower reactivity, not very different from the reactivity of negative sera (NS) from a bank of samples collected before 2019. The six best spike binders also proved to be the most potent at inhibiting the interaction of spike with ACE2 (**Figure 1b, bottom panel**) and the best to neutralize viral infectivity in Vero E6 cells (**Table 1**). Based on sera screening, total RNA was extracted from lymphocytes of the six best donors, converted in cDNA and immunoglobulin genes were amplified and cloned in scFv antibody format for phage display, as depicted in **Supplementary Figure 1a**. After selection cycles by panning, RBD best binders were subjected to affinity maturation followed by repeated panning on RBD under stressing conditions (low antigen concentration, washing at low pH, high temperature). Selected scFv5, scFv86 and scFv76 antibodies, as well as affinity matured derivatives from scFv76 (scFv76-46, scFv76-55, scFv76-57, scFv76-58 and scFv76-77) coded as scFv76-cluster were produced in a soluble form and purified according to the procedure schematized in **Supplementary Figure 1b**. All soluble scFv antibodies were found able to bind to the spike protein of the original Wuhan strain at concentrations in the low nanomolar range (data not shown). Amino acid sequences of CDR3 and immunoglobulin germline usage of the selected scFv antibodies are shown in **Table 2**. The scFv76-cl Abs share VH CD3 <u>ARDLSVAGAFDI</u> which is derived from the IGVH3-53 germline with minor differences in the remaining VH sequence. Diversity is contributed by VL sequences which are derived from

bioRxiv preprint doi: https://doi.org/10.1101/2021.06.04.447066; this version posted June 4, 2021. The copyright holder for this preprint (which was not certified by peer review) is the author/funder. All rights reserved. No reuse allowed without permission.

IGVK3-20 germline except for scFv76-55 and scFv76-57 antibodies that use VL CDR3 derived from IGVK3-15 and IGVK1-9 germline, respectively. On the other hand, scFv5 and scFv86 antibodies share identical IGVH1-46-derived VH CDR3 and IGVL2-14 and IGVK3-11 derived VL CD3, respectively.

Recombinant spike proteins representative of the current SARS-CoV-2 VOCs were further used to test antibody reactivity. In particular, we included: (1) spike containing mutation D614G, here indicated as S1(D614G) now present in most viral isolates; (2) spike bearing HV69-70del, Y144del, N501Y, A570D, D614G, P681H indicated as S1(UK), described as the UK VOC; (3) spike with mutations at K417, E484, N501 and D614, here indicated as S1(SA-BR), representing the South Africa and Brazil VOCs. These variants were used to assess binding, affinity and inhibition of spike/ACE2 interaction. Results in **Figure 1c** show that all scFv antibodies, except for scFv76-55 which loses reactivity against S1(SA-BR), are resilient in their binding to the spike variants. Binding analysis of scFv antibodies was extended to single RBD mutations. Results shown in **Supplementary Figure 2** indicate that single mutations differently affect the binding capacity of antibodies with scFv76-55, scFv5 and scFv86 being the most sensitive to RBD mutations. The nM concentration to yield 1.0 OD was calculated to compare the binding of scFv antibodies on all mutated SARS-CoV-2 spike and RBD proteins and data, reported in **Table 3,** confirm that the scFv76-cl Abs strongly bind spike variants and mutated RBD, with the exception of scFv76-55 antibody that showed reduced binding to spike proteins carrying mutations N439K, A475V and E484K, the latter position being mutated in both SA and BR variant spikes. Again, the scFv5 and scFv86 antibodies recognized less efficiently all mutated spikes when compared with the scFv76-cl Abs. In addition, scFv5 and scFv86 loss of binding to spike carrying mutations V483A and I472V suggests recognition of a different RBD epitope.

In a set of independent experiments, affinity of scFv antibodies for SARS-CoV-2 spike was measured by Surface Plasmon Resonance (SPR). Representative results of the scFv76 in **Figure 1d**

bioRxiv preprint doi: https://doi.org/10.1101/2021.06.04.447066; this version posted June 4, 2021. The copyright holder for this preprint (which was not certified by peer review) is the author/funder. All rights reserved. No reuse allowed without permission.

indicate identical subnanomolar affinity for S1(D614G) and S1(UK) and lower affinity for the S1(SA-BR) that, however, is still in the low nanomolar range. Sensorgrams of all scFv antibodies on the three spike variants are shown in **Supplementary Figure 3.** Faster dissociation from S1(SA-BR) was observed for the scFv76-55 antibody. Kinetic data of all antibodies are reported in **Table 4** showing K_D values ranging between subnanomolar and 1-digit nanomolar concentrations, except for scFv76-55 that exhibits a K_D of 14.9 nM for S1(SA-BR). Kinetic data of all antibodies on RBD single mutations are reported in **Supplementary Table 1**. In additional SPR experiments we found that the six scFv76-cl Abs, sharing the same VH CDR3, do not show additive binding properties, suggesting that they might recognize the same or a very close antigenic epitope, while scFv5 binds to an independent epitope (**Figure 1e**). Similar results were obtained with scFv86 (not shown).

In order to test the ability of the scFv76-cl Abs to recognize a SARS-CoV-2 native spike, HEK293T cells were transfected with a spike-encoding plasmid (Wuhan strain). High content screening (HCS) fluorescent imaging was used to visualize the specific scFv76 antibody binding to HEK293T spike+ cells (**Figure 1f**). Similar data (not shown) were obtained with the other scFv76-cl Abs. These results were confirmed by cytofluorimetry indicating the ability of such antibodies to recognize the spike when expressed on the cell surface (data not shown).

In vitro studies of the inhibitory effects of SARS-CoV-2 spike binding to ACE2

In a prospective development of scFv76-cl Abs as antiviral drug candidates, they were evaluated for their ability to inhibit the binding of the viral spike to the human ACE2 receptor and for their capacity to neutralize viral infectivity. Results in **Figure 2a** show that scFv76-cl Abs, but not antibodies scFv5 and scFv86, inhibit the interaction of S1(D614G), S1(UK) or S1(SA-BR) with ACE2, except for scFv76-55. Consistently with binding data, inhibition activity of scFv76-55 is the most affected by the SA-BR mutations. Data on the effect of single RBD mutations on inhibition by

bioRxiv preprint doi: https://doi.org/10.1101/2021.06.04.447066; this version posted June 4, 2021. The copyright holder for this preprint (which was not certified by peer review) is the author/funder. All rights reserved. No reuse allowed without permission.

scFv antibodies of the binding to ACE2 are shown in **Supplementary Figure 4.** These data identify A475V and K417N as the most critical mutations affecting scFv76-55 binding. The IC_{50} (expressed in nM) to ACE2 as assessed using an ELISA assay of all spike variants and of single RBD mutations is reported in **Table 5.** Interestingly and consistently with binding and SPR affinity data, these results indicate that the scFv76-cl Abs, except for scFv76-55, maintain the capacity to strongly inhibit the binding of spike variants and mutated RBD to ACE2.

Neutralization of SARS-CoV-2 infectivity by scFv76-cl Abs was then tested by micro-neutralization assay of cytopathic effect (CPE) in Vero E6 cells. All scFv76-cl Abs proved to be effective with MN50 (50% microneutralization titer) <15 nM (**Figure 2b**).

Viral neutralization potency of scFv76, scFv76-46 and scFv76-58 antibodies was then evaluated in human pulmonary Calu-3 cells infected with SARS-CoV-2 WT (Wuhan strain), D614G or UK variants and analyzed by RT-qPCR. Results in **Table 6** show that scFv antibodies, added to the cell culture 1 h after the infection, are effective at inhibiting all virus strains with IC_{50} concentrations <22 nM. When antibodies were added 1 h before infection the concentration to obtain 50% viral inhibition was below 2.2 nM. Under the same experimental conditions, IC_{50} dilutions of positive sera (pool of the six best responder sera from COVID-19 convalescent subjects of Figure 1b and Table 1), were >1/200 and >1/10.000 when added 1 h after or before infection, respectively.

To extend the investigation of potential viral escape of variants to the neutralization capacity of scFv76-cl Abs, human colon Caco-2 cells stably expressing the human ACE2 (hACE2) receptor (Caco-2 hACE2) were infected with luciferase-expressing SARS-CoV-2 S-pseudoviruses bearing single (D614G or N501Y) or triple (K417N, E484K, N501Y) mutations. Results in **Figure 2c-e** confirm that all scFv76-cl Abs, but not scFv5, inhibit all pseudovirus variants infection and that, consistently with previous data, scFv76-55 antibody was less effective and the most sensitive to mutations.

bioRxiv preprint doi: https://doi.org/10.1101/2021.06.04.447066; this version posted June 4, 2021. The copyright holder for this preprint (which was not certified by peer review) is the author/funder. All rights reserved. No reuse allowed without permission.

In further experiments designed to investigate the ability of scFv76-cl Abs to prevent SARS-CoV-2 spike-induced syncytia formation, a pathognomonic feature of pulmonary COVID-19 (*9*), the scFv76 antibody proved to be strongly effective at inhibiting cell-cell fusion between Wuhan (WT) spike- or D614G spike-expressing human HEK293T cells and human lung A549 cells stably expressing the human ACE2 receptor (A549 hACE2), or monkey Vero E6 cells (**Figure 3a and b; Supplementary Figure 5**).

Spike antigenic epitope of scFv76 antibody

Identification of the epitope recognized by the anti-SARS-CoV-2 scFv76 antibody was performed by shotgun mutagenesis (alanine scanning) and binding analysis by high-throughput flow cytometry of each mutated protein expressed in human cells in comparison with the Wuhan (WT) spike clone. Because of high affinity of the scFv76 antibody for its target, high stringency (HS) conditions were applied in the screening including combinations of increased pH, salinity, temperature, and/or increased washing time.

Results in **Figure 4a** indicate reactivity loss of scFv76 antibody, but not of mAb CoV16 (a control antibody directed against an independent RBD epitope), towards 5 mutated SARS-CoV-2 spike proteins with alanine substituted to residues L455, F456, Y473, N487 and Y489. Percent of the respective binding reactivity is shown in **Figure 4b**. These residues are within the spike RBM with F456 being the most critical mutation for the scFv76 antibody spike recognition. **Figure 4c and d** visualize the critical residues (red spheres) on a crystal of the SARS-CoV-2 spike protein trimer (*10*) (PDB ID # 6XCN) and the SARS-CoV-2 spike protein receptor binding domain (*11*) (PDB ID# 6Z2M), respectively.

bioRxiv preprint doi: https://doi.org/10.1101/2021.06.04.447066; this version posted June 4, 2021. The copyright holder for this preprint (which was not certified by peer review) is the author/funder. All rights reserved. No reuse allowed without permission.

Biochemical and structural characterization of scFv76-cluster antibodies

The molecular size of scFv76-cl Abs was analyzed by SDS-PAGE and results are reported in **Supplementary Figure 6a**. All antibodies showed an apparent molecular weight of about 28 kDa, as expected based on deduced amino acid sequence. Molecular integrity was then analyzed by size exclusion chromatography (SEC-HPLC). Representative chromatogram of the scFv76 antibody is shown in **Figure 5a**. Chromatograms of all remaining scFv76-cl Abs are given in **Supplementary Figure 6b**. In most cases, the SEC-HPLC analysis shows chromatographic profiles with a major peak compatible with the antibody monomeric form and minor additional peaks of variable area compatible with dimeric/multimeric species. Such species were found more represented when chromatography was run without 10% acetonitrile (not shown). Coexistence of both monomeric and dimeric species in scFv antibody preparations has been known for decades as a peculiarity of this type of proteins (*12,13*).

Molecular weight of scFv antibodies was further confirmed by SEC-HPLC-mass spectrometry (MS) using 20mM ammonium formate as native elution buffer. The average spectrum obtained from all MS spectra of the scFv76 antibody, between 5 and 7 minutes, is reported in **Figure 5b** where two gaussian dispersions, centered on m/z 2800 and m/z 4000, are present. Their deconvolution indicates the presence of two species with molecular weight 28008 and 56016 that correlate with scFv76 monomeric and dimeric forms, respectively. The result of peptide mapping performed by trypsin digestion of scFv76 followed by Reverse Phase-Ultra-HPLC-MS/MS analysis is shown in **Figure 5c** that confirms 100% matching of scFv76 peptides with the expected amino acidic sequence. Similar results were obtained with scFv76-46, scFv76-58 and scFv76-77 (not shown).

Thermal resistance, selected as a surrogate marker of protein stability, was then investigated. The scFv76-cl Abs were subjected to high temperature stress by heating solutions for 1 h at increasing temperatures and testing for antigen binding by ELISA. Results in **Figure 5d** indicate

bioRxiv preprint doi: https://doi.org/10.1101/2021.06.04.447066; this version posted June 4, 2021. The copyright holder for this preprint (which was not certified by peer review) is the author/funder. All rights reserved. No reuse allowed without permission.

scFv76-57 as the most sensitive to high temperature loosing completely antigen binding properties upon incubation at 59 °C while all other antibodies appear to be more stable to heating with scFv76, scFv76-46 and scFv76-58 being the most resistant proteins of the scFv76-cluster.

To assess protein folding and secondary structure content, far-UV circular dichroism (CD) spectra of scFv76-cl Abs were recorded at 20 and 90 °C (**Figure 5e and Supplementary Figure 7**). CD spectra of antibodies at 20 °C resemble those of folded proteins with significant β-sheet content, while the spectra at 90 °C show that the antibodies have undergone unfolding. Quantitative analysis of CD spectra at 20 °C, by means of BeStSel (*14*), indicates that the scFv76-cl Abs have a folded structure with about 40% of antiparallel β-sheet content (**Supplementary Table 2**).

From thermal stability experiments scFv76, scFv76-46 and scFv76-58 appear to be the most resistant while scFv76-57 appears to be the most sensitive. Considering the prospective clinical use of scFv76-cl Abs by intranasal drops/spray or aerosol, we also addressed their stability to nebulization. Antibodies nebulized by using Aeroneb Lab Nebulizer system (EMKA, Aerogen) were analyzed by SEC-HPLC and ELISA. Results indicate that nebulization affects neither protein structure nor the capacity to inhibit RBD interaction with ACE2 of scFv76-cl Abs and similar results were obtained with antibody preparations reconstituted after lyophilization (data not shown).

Intranasal administration of scFv76 antibody counteracts viral infection in animal models

To test the efficacy of scFv76 antibodies against SARS-CoV-2 infection, a model of human ACE2-expressing transgenic (tg) mice was used. Tg mice were infected with a luciferase-expressing D614G S-pseudotyped virus and infection was measured by bioluminescence imaging (BLI). **Figure 6a** shows representative BLI images of two animals out of 5/group at different time points indicating that the intranasal administration of 74 µg/mouse of scFv76, 2 h before and 4 h after infection, completely blocks the virus as deduced by loss of luminescent signal. Quantitative BLI

bioRxiv preprint doi: https://doi.org/10.1101/2021.06.04.447066; this version posted June 4, 2021. The copyright holder for this preprint (which was not certified by peer review) is the author/funder. All rights reserved. No reuse allowed without permission.

data in nasal turbinates are shown in **Figure 6b**. In a confirmatory study also scFv76-58 as well as an unrelated scFv antibody were tested. Results in **Figure 6c** confirm the efficacy of scFv76 and show efficacy of scFv76-58 and no activity of the unrelated antibody, thus proving the treatment specificity.

In a further study, hamsters infected with SARS-CoV-2 virus (D614G strain) and intranasally treated with 70 µg of scFv76, 2 h before and once daily for the two consecutive days post infection, were protected from body weight loss compared to the animals treated with vehicle (**Figure 6d**). This result correlated with reduction of nasal discharge (**Figure 6e**) and with reduction of gross pathology marks in the lung (i.e. red and brown spots) at necropsy (not shown).

Discussion

Herein we describe a cluster of six human scFv antibodies sharing a unique VH CDR3 sequence and recognizing a conserved epitope of the SARS-CoV-2 spike protein.

Human scFv antibodies, compared to small size single-domain VHH antibodies (12-15 kDa), may be more advantageous for the development of therapeutics because of the need for VHH of sophisticated humanization procedures (*15*) or cumbersome immunogenicity testing (*16*) related to their camelid origin.

The scFv76 antibodies here described recognize an invariant epitope within the human ACE2 RBM. Such epitope consists of residues L455, F456, Y473, N487, Y489, which are, to date, not listed among SARS-CoV-2 VOCs, VOIs or VUIs (SARS-CoV-2 Variant Classifications and Definitions (cdc.gov) and **Supplementary Figure 8**), thus suggesting that this epitope may be essential for maintaining the docking efficiency of RBD to ACE2. Additionally, it is to note that the scFv76-cluster antibody reactivity is not significantly affected by mutations at residues K417, L452, E484, N501 and D614, which are found singularly or combined in the most threatening spike VOCs

bioRxiv preprint doi: https://doi.org/10.1101/2021.06.04.447066; this version posted June 4, 2021. The copyright holder for this preprint (which was not certified by peer review) is the author/funder. All rights reserved. No reuse allowed without permission.

and lineages of SARS-CoV-2 variants including B.1.427 and B.1.429 found in California (USA) and B1.1.7, P1, B1.351 found in South Africa, Brazil and UK (CDC, 2021). Intriguingly, mAbs Bamlanivimab (LY-CoV555) and casirivimab (REGN10933) were recently found to be unable to block viral variants bearing the E484K mutation in RBD (*17*), thus making these products unsuitable for the treatment of South Africa (B.1.351 lineage) or Brazil (B.1.128.1 lineage) emerging infections. More recently, mutation L452R was found combined with E484Q in VUI B.1.617 in India. Based on present data, we expect the neutralizing activity of scFv76-cl Abs to be maintained since both mutations were found to be independently recognized. Similarly, the recently described SARS-CoV-2 VUI B.1.620, found in several European states and in central Africa (*18*), is expected not to escape scFv76-cluster antibody recognition. In fact, this variant carries two spike mutations that are either already shown to be recognized (E484K) or are not among the residues composing the spike antigenic epitope (S477N).

However, not all scFv antibodies of the scFv cluster showed the same features. In particular, the scFv76-55 antibody stands out for lower binding affinity against all mutated spike proteins and lower potency at inhibiting the interaction of SARS-CoV-2 spike with ACE2. Further structural analysis of the scFv76 cluster may help in understanding this different behavior.

The scFv76-cl Abs share an identical VH CDR3 sequence, which is derived from the IGVH3-53 germline. The scFv76, scFv76-46, scFv76-58 and scFv76-77 antibodies also share similar VK CDR3 from IGVK3-20 germline, while scFv76-55 and scFv76-57 have different VK sequences. The scFv76-cl Abs pairing VH3-53-derived heavy chain with VK3-20-derived light chain exhibit the highest affinity for RBD and the highest potency at inhibiting RBD interaction with ACE2 and viral infectivity.

A recently described mAb, C102, also using VH3-53-derived VH sequences paired with VK3-20-derived VK sequences, was found to recognize the spike RBD in the up conformation with a K_D=27 nm (*19*). Affinity of the C102 antibody was reduced approximately 15- and 2-folds in the

bioRxiv preprint doi: https://doi.org/10.1101/2021.06.04.447066; this version posted June 4, 2021. The copyright holder for this preprint (which was not certified by peer review) is the author/funder. All rights reserved. No reuse allowed without permission.

presence of RBD mutation at positions A475V and E484K, respectively. Interestingly, scFv76-cl Abs, exhibiting affinity for WT RBD proteins in the range of subnanomolar-1digit nanomolar K_D, substantially maintain their affinity towards mutated RBD. Moreover, loss of affinity of scFv76-cl Abs towards mutated RBD at position A475V is significantly lower than that of C102 antibody despite identical germline origin.

Binding and affinity data identify scFv76-cl Abs as suitable neutralizing candidates of WT and mutated SARS-CoV-2 spike proteins, as also confirmed by viral neutralization experiments of pseudotyped and natural viruses. We also show that the efficient neutralization of RBD interaction with ACE2 by scFv76-cl Abs translates into striking inhibition of SARS-CoV-2 S-mediated cell-cell fusion in human lung cells *in vitro*. This result is particularly interesting as the syncytia formation in pneumocytes is a hallmark of COVID-19, driving life-threatening localized thromboembolism and inflammation (*9*,*20*).

Finally, we obtained evidence of *in vivo* neutralizing potential of intranasal topical administration of scFv76-cl Abs in both transgenic mice expressing human ACE2 and hamsters. The intranasal administration is clinically attractive and possibly complementary to the intravenous dosing route. A recent work in fact reported persistent high SARS-CoV-2 presence in nasal turbinates after treatment with systemic neutralizing antibodies (*21*).

In summary, all properties of the scFv antibodies herein described, and particularly their ability to recognize an essential and apparently unalterable spike antigenic epitope, are compatible with the development of pharmaceutical preparations to prevent and counteract SARS-CoV-2 infection by intranasal and/or aerosol delivery. To our knowledge, this is the first example of drug candidates in the human scFv antibody format for COVID-19 treatment.

bioRxiv preprint doi: https://doi.org/10.1101/2021.06.04.447066; this version posted June 4, 2021. The copyright holder for this preprint (which was not certified by peer review) is the author/funder. All rights reserved. No reuse allowed without permission.

Acknowledgments

We are grateful to Integral Molecular, Philadelphia, USA for expedite identification of the antibody epitope; Dr. Silvia Santopolo for help with pseudovirus RNA titration; Dr Nestor Santiago Gonzalvo (Cytiva) for excellent technical assistance on Biacore analyses; Mr Claudio Albertoni and Mrs Evelyn Vaccaro for expert technical assistance in animal models.

Author contribution

OM and DS generated libraries, selected and purified scFv antibodies; FM coordinated in vitro and in vivo activity studies; AMA characterized patient sera and scFv antibodies for antigen binding and inhibition of RBD/ACE2 interaction; GB[1] coordinated biochemical analyses; CC, AR[1] contributed to characterization of scFv antibodies; EMP contributed to the discussion; GG, GB[2], AR[2,3] identified convalescent patients and purified RNA from lymphocytes; CD, CV studied neutralization of SARS-CoV-2 by TCID; BP contributed with CD analyses; LS performed peptide mapping; AR[8] performed experiments with pseudovirus; EM, LL performed in vivo studies with pseudovirus; GS, AR[9] studied scFv inhibition of syncytia formation; RDS designed the study, supervised experiments and wrote the manuscript.

Competing Interests

OM, EMP and RDS are employees of Alfasigma SpA and are named as inventors on a patent application on the name of the same Company. Patent application is related to scFv76-cluster antibody sequences and to the use of scFv antibodies encoded by such sequences as drugs for prevention and treatment of COVID-19.

bioRxiv preprint doi: https://doi.org/10.1101/2021.06.04.447066; this version posted June 4, 2021. The copyright holder for this preprint (which was not certified by peer review) is the author/funder. All rights reserved. No reuse allowed without permission.

Figure legends

Figure 1. Selection of anti-SARS-CoV-2 spike RBD-specific human scFv antibodies

a, Flow chart of experimental steps; **b**, Representative analysis of 10 COVID-19 convalescent sera (CS) and negative sera collected from donors before 2019 (NS), for binding to spike and inhibition of spike/ACE2 interaction by ELISA. Data are expressed as the dilution giving 0.5 OD (λ = 450 nm) and IC_{50} dilution, respectively; **c**, Binding of scFv antibodies to spike S1(D614G) or spike S1(UK) bearing HV69-70d, Y144d, N501Y, A570D, D614G, P681H mutations or spike S1(SA-BR) with mutations K417N, E484K, N501Y, D614G, assessed by ELISA. Data are the average (± SD) of three technical replicates from one representative experiment; **d**, SPR sensorgrams of scFv76 antibody on spikes as in c; **e**, SPR epitope binning by injection of scFv76 antibody followed by indicated scFv antibodies; **f**, High content screening immunofluorescence imaging (Operetta) of spike-transfected HEK293T cells incubated with scFv76 antibody. Binding detected by FITC-conjugated anti-tag antibody. Inset, mock transfected cells.

Figure 2. *In vitro* functional characterization of anti-SARS-CoV-2 human scFv antibodies

a, Inhibition of spike/ACE2 interaction by scFv antibodies measured by ELISA. Data are expressed as % inhibition and are the average (± SE) of 2-3 independent experiments; **b**, Neutralizing activity of scFv antibodies assessed by viral titration (Wuhan strain) in Vero E6 cells by TCID50 assay; **c-e**, Neutralization of SARS-CoV-2-S pseudoviruses bearing the spike D614G mutation (**c**), a single mutation at position N501Y (**d**), or multiple mutations at position K417N, E484K, N501Y (**e**) by scFv antibodies, assessed by luciferase assay in hACE2-expressing Caco-2 cells, 72 h after infection. Data, expressed as percentage of infection relative to control, represent the average (±SD) of two independent replicates from one representative experiment.

bioRxiv preprint doi: https://doi.org/10.1101/2021.06.04.447066; this version posted June 4, 2021. The copyright holder for this preprint (which was not certified by peer review) is the author/funder. All rights reserved. No reuse allowed without permission.

Figure 3. scFv76 antibody inhibits SARS-CoV-2 spike-mediated cell-cell fusion

a,b, HEK293T cells (donor cells) co-transfected with plasmids encoding the SARS-CoV-2 spike Wuhan (wild type, WT) (**a**) or carrying the D614G mutation (**b**) and GFP, or empty vector and GFP (Mock) were detached at 40 h post transfection, incubated for 1 h with scFv76 or scFv5 antibodies (10 µg/mL) in culture medium, and then overlaid on monolayers of human lung A549 cells stably expressing the hACE2 receptor (A549-hACE2 cells) (target cells). After 4 h, transmission and fluorescence images were taken using a ZEISS Axio Observer inverted microscope. Merge and zoom images are shown. Scale bar, 200 µm (zoom, 50 µm). Cell-cell fusion was determined and expressed as percentage relative to control (bottom panels). Data represent average (±SD) of 5 fields from two biological replicates. *P<0.0001; ANOVA test.

Figure 4. Epitope mapping of anti-SARS-CoV-2 scFv76 antibody

a, Identification of critical clones for scFv76 binding. Binding to each mutant clone in the alanine scanning library was determined, in duplicate, by high-throughput flow cytometry. For each point, background fluorescence was subtracted from the raw data, which were then normalized to scFv76 reactivity with WT target protein. For each mutant clone, the mean binding value was plotted as a function of expression (represented by control reactivity). To identify preliminary primary critical clones (red circles), a threshold (dashed lines) of >65% WT binding to control Ab and <25% WT binding to test Abs was applied. **b**, Mean binding reactivities (and ranges) are listed for all identified critical residues. Critical residues for Ab binding (outlined in red) were residues whose mutations were negative for binding to scFv76 but positive for binding to control antibody. **c**, Visualization of critical residues for scFv76 binding on crystal structure of the SARS-CoV-2 spike protein trimer (PDB ID # 6XCN) and **d**, on SARS-CoV-2 spike protein receptor binding domain (PDB ID # 6Z2M).

bioRxiv preprint doi: https://doi.org/10.1101/2021.06.04.447066; this version posted June 4, 2021. The copyright holder for this preprint (which was not certified by peer review) is the author/funder. All rights reserved. No reuse allowed without permission.

Figure 5. **Biochemical and structural characterization of scFv76-cluster antibodies**

a, UV chromatogram at 280 nm from SEC-HPLC analysis of scFv76 in 50 mM phosphate buffer, 150 mM NaCl, 10% acetonitrile, pH 7.2 on BioSep SEC-s2000 (Phenomenex) column; **b**, Total ionic current (TIC) chromatogram from SEC-HPLC analysis of scFv76 in 20 mM ammonium formate, pH 6.8 on Mab Pac SEC-1 column (Thermo). Inset, mass spectrum as average of spectra recorded between 5 and 7 min; **c**, scFv76 sequence coverage by peptide mapping after trypsin digestion; **d**, Binding of thermally stressed scFv76-cluster antibodies to spike by ELISA; **e**, Far-UV CD spectra of scFv76 in PBS buffer recorded at 20 (solid line) and 90 °C (dashed line).

Figure 6. ScFv76 antibody inhibits viral infectivity in animal models by intranasal administration

a, Representative bioluminescence (BLI) images of 2 out of 5 human ACE2-expressing transgenic (K18-hACE2) mice infected with luciferase-expressing SARS-CoV-2 spike (D614G) pseudotyped virus and intranasally treated with 74 µg/mouse scFv76 antibody, 2 h before and 4 h after infection. BLI imaging was recorded at indicated time points by the Xenogen IVIS 200 Imaging System; **b**, Average of light photons/sec measured in mice nasal turbinates of study in **a**. Data are the average (± SE) of 5 animals. Student's t-test versus vehicle-treated mice; **$p < 0.01$; **c**, Experimental setting as in **a**, also including scFv76-58 and an unrelated scFv antibody. Total body BLI data are the average (± SE) of 5 animals at indicated time points. Student's t-test versus vehicle-treated mice; ***$p < 0.001$. **d**, Female hamsters were intranasally infected with SARS-CoV-2 strain "Slovakia/SK-BMC5/2020" with D614G mutation (10^5 pfu/animal) on day 0. Two h before infection and then once daily for 2 subsequent days post-infection animals (n=5) were administered intranasally with 70 µg in 70 µL (35 µL/nostril) scFv76 antibody or with equivalent volumes of vehicle. Control animals were only infected but not treated. Body weight was daily recorded, and results expressed as % versus day 0 body weight. Data are the average (± SD) of 5 animals. **e**,

bioRxiv preprint doi: https://doi.org/10.1101/2021.06.04.447066; this version posted June 4, 2021. The copyright holder for this preprint (which was not certified by peer review) is the author/funder. All rights reserved. No reuse allowed without permission.

Assessment of nasal discharge from animals of study in **d.** Results are expressed as score (inset table).

Table 1 Viral neutralization by COVID-19 convalescent sera

	MN50		
CS6	1/100		
CS9	1/100		
CS10	1/100		
CS8		1/50	
CS1		1/50	
CS4		1/50	
CS2			Undetected
CS5			Undetected
CS3			Undetected
NS pool			Undetected

Neutralizing activity against SARS-CoV-2 (Wuhan strain) of sera from 10 COVID-19 convalescent patients by micro-neutralization assay in Vero E6 cells. Sera were decomplemented for 30 min at 56 °C and then added to cells after 2-fold dilutions ranging from 1/50-1/800 (8 replicates). Cytopathogenic effect (CPE) was measured after 4 days cultivation. Data are expressed as the titer (dilution) at which no CPE was observed in at least half of wells (50% micro-neutralization titer, MN50) calculated according to the Spearman-Kärber formula.

Table 2 Sequence alignment CDR3 of heavy and light chain and germline usage of anti-SARS-CoV-2 human scFv antibodies

ScFv	VH CDR3	Germline	VL CDR3	Germline
76	ARDLSVAGAFDI	IGVH3-53	QQYGSSP_YT	IGVK3-20
76-46	ARDLSVAGAFDI	IGVH3-53	QQYGSSP_IT	IGVK3-20
76-55	ARDLSVAGAFDI	IGVH3-53	QQYVRSP_PT	IGVK3-15
76-57	ARDLSVAGAFDI	IGVH3-53	QHRD_____I	IGVK1-9
76-58	ARDLSVAGAFDI	IGVH3-53	QQYGSSPRIT	IGVK3-20
76-77	ARDLSVAGAFDI	IGVH3-53	QEYGSSPRVT	IGVK3-20
5	ATGGAVPHVTGAFDI	IGVH1-46	NSYTRFSTGV	IGVL2-14
86	ATGGAVPHVTGAFDI	IGVH1-46	QQRSNWPPGFT	IGVK3-11

Sequence alignment was performed by IGBLAST tool https://www.ncbi.nlm.nih.gov/igblast/

Table 3 Binding of anti-SARS-CoV-2 scFv antibodies to spike and RBD mutants

	Spike				RBD										
ScFv	**WT**	**D614G**	**UK**	**SA-BR**	**WT**	**N501Y**	**V483A**	**I472V**	**Y453F**	**A475V**	**E484K**	**N439K**	**A520S**	**L452R**	**K417N**
76	0.25(0.11)	0.14(0.04)	0.21(0.14)	0.54(0.29)	0.11(0.04)	0.11(0.04)	0.21(0.11)	0.21(0.11)	0.11(0.04)	0.43(0.14)	0.54(0.04)	0.25(0.21)	0.14(0.04)	0.11(0.04)	0.14(0.04)
76-46	0.29(0.11)	0.14(0.04)	0.29(0.21)	0.61(0.36)	0.18(0.07)	0.18(0.00)	0.32(0.18)	0.36(0.18)	0.18(0.07)	0.54(0.29)	0.64(0.04)	0.36(0.25)	0.32(0.11)	0.29(0.14)	0.18(0.04)
76-55	0.57(0.40)	0.25(0.14)	0.43(0.04)	>10xWT	0.14(0.04)	0.32(0.22)	0.79(1.01)	0.83(1.08)	0.32(0.25)	>10xWT	>10xWT	>10xWT	0.32(0.22)	0.29((0.18)	0.32(0.04)
76-57	0.51(0.36)	0.25(0.15)	0.44(0.04)	1.34(0.76)	0.18(0.07)	0.33(0.22)	0.58(0.65)	0.62(0.73)	0.33(0.22)	1.12(1.12)	1.12(0.58)	1.34(1.45)	0.33(0.22)	0.29(0.22)	0.36(0.04)
76-58	0.39(0.21)	0.25(0.11)	0.32(0.21)	0.89(0.46)	0.21(0.07)	0.21(0.04)	0.39(0.28)	0.60(0.64)	0.21(0.04)	0.60(0.21)	1.64(0.64)	0.85(0.82)	0.25(0.11)	0.25(0.07)	0.18(0.00)
76-77	0.25(0.04)	0.18(0.04)	0.21(0.14)	0.43(0.14)	0.11(0.04)	0.11(0.00)	0.28(0.11)	0.25(0.14)	0.14(0.04)	0.32(0.21)	0.43(0.14)	0.28(0.21)	0.21(0.07)	0.18(0.04)	0.14(0.00)
5	2.91(1.49)	1.06(0.32)	1.70(1.74)	4.79(4.58)	1.06(0.32)	3.19(1.92)	>10xWT	>10xWT	3.09(0.75)	>10xWT	>10xWT	>10xWT	1.06(0.50)	1.77(0.92)	1.99(0.00)
86	1.77(1.17)	0.71(0.28)	1.03(0.78)	3.16(2.45)	0.60(0.25)	1.38(0.18)	>10xWT	>10xWT	1.42(0.21)	>10xWT	>10xWT	>10xWT	0.75(0.50)	0.85(0.53)	0.96(0.11)

Binding of scFv antibodies to SARS-CoV-2 spike and RBD variants measured by ELISA. Data are expressed as nM concentration to have 1.0 OD (λ 450 nm) and are the average (±SD) of 2-3 independent experiments. WT (Wuhan strain). Spike with mutations HV69-70d, Y144d, N501Y, A570D, D614G, P681H (UK) or spike with mutations K417N, E484K, N501Y, D614G (SA-BR). Boxed numbers indicate fold increase >10x versus WT.

bioRxiv preprint doi: https://doi.org/10.1101/2021.06.04.447066; this version posted June 4, 2021. The copyright holder for this preprint (which was not certified by peer review) is the author/funder. All rights reserved. No reuse allowed without permission.

Table 4 Affinity of anti-SARS-CoV-2 scFv antibodies for spike protein variants by Surface Plasmon Resonance

scFv	Spike S1	k_a (10^5 M^{-1} s^{-1})	k_d (10^{-5} s^{-1})	K_D (nM)
76	WT	1.4	4.7	0.3
	S1(D614G)	1.3	6.0	0.4
	S1(UK)	1.1	4.3	0.4
	S1(SA-BR)	1.1	50.0	4.5
76-46	WT	1.9	3.1	0.2
	S1(D614G)	1.9	4.8	0.3
	S1(UK)	1.4	7.3	0.5
	S1(SA-BR)	1.1	83.7	7.7
76-55	WT	1.4	42.1	3.0
	S1(D614G)	1.5	39.9	2.7
	S1(UK)	1.2	61.6	5.1
	S1(SA-BR)	1.5	223.0	14.9
76-57	WT	1.5	7.6	0.5
	S1(D614G)	1.5	6.7	0.4
	S1(UK)	1.1	10.6	0.9
	S1(SA-BR)	1.5	49.5	3.3
76-58	WT	2.8	32.6	1.1
	S1(D614G)	3.3	34.7	1.1
	S1(UK)	2.8	34.0	1.2
	S1(SA-BR)	1.7	75.0	4.5
76-77	WT	1.5	3.0	0.2
	S1(D614G)	1.4	4.9	0.3
	S1(UK)	1.4	2.0	0.1
	S1(SA-BR)	1.1	31.6	2.8
5	WT	0.5	19.8	4.3
	S1(D614G)	0.4	17.5	4.4
	S1(UK)	0.5	19.8	4.2
	S1(SA-BR)	0.5	20.0	4.1
86	WT	0.7	9.6	1.5
	S1(D614G)	0.6	11.4	1.8
	S1(UK)	0.7	11.2	1.7
	S1(SA-BR)	0.7	11.5	1.6

Table 5 Inhibitory activity (IC_{50}) of anti-SARS-CoV-2 scFv antibodies on spike or RBD binding to human ACE2

	Spike				RBD										
scFv	**WT**	**D614G**	**UK**	**SA-BR**	**WT**	**N501Y**	**V483A**	**I472V**	**Y453F**	**A475V**	**E484K**	**N439K**	**A520S**	**L452R**	**K417N**
76	0.62(0.11)	1.11(0.07)	1.07(0.21)	1.84(0.14)	0.67(0.1)	1.20(0.14)	1.29(0.11)	1.18(0.17)	2.16(0.14)	1.74(0.24)	0.88(0.16)	1.37(0.11)	1.04(0.07)	0.91(0.07)	1.63(0.56)
76-46	0.54(0.05)	1.23(0.12)	1.72(0.25)	1.94(0.09)	1.22(0.21)	1.55(0.08)	2.20(0.12)	1.44(0.31)	1.93(0.13)	1.92(0.30)	1.15(0.38)	1.11(0.06)	1.31(0.12)	1.16(0.34)	1.79(0.58)
76-55	1.87(0.15)	2.65(0.15)	2.94(0.37)	>40	2.03(0.32)	2.71(0.09)	2.98(0.16)	1.99(0.02)	3.57(0.38)	3.45(0.40)	1.77(0.14)	2.09(0.34)	2.19(0.27)	1.84(0.31)	2.59(0.36)
76-57	1.61(0.24)	2.49(0.16)	2.56(0.13)	2.63(0.34)	2.09(0.15)	2.59(0.25)	2.49(0.17)	2.42(0.25)	2.83(0.19)	4.30(1.11)	2.00(0.04)	2.05(0.33)	2.18(0.24)	2.27(0.08)	1.98(0.31)
76-58	0.77(0.12)	1.44(0.21)	1.73(0.09)	2.74(0.21)	1.45(0.21)	1.74(0.12)	1.48(0.24)	1.54(0.12)	2.31(0.15)	3.91(1.00)	2.06(0.11)	1.42(0.27)	1.50(0.17)	1.74(0.15)	1.76(0.59)
76-77	0.36(0.08)	0.72(0.15)	0.90(0.13)	1.62(0.16)	0.58(0.04)	0.78(0.16)	0.77(0.21)	1.19(0.07)	1.36(0.07)	1.69(0.19)	0.97(0.16)	1.14(0.32)	0.79(0.08)	0.88(0.08)	1.67(0.75)

Competition of scFv antibodies in spike or RBD binding to human ACE2 measured by ELISA. IC_{50} values (expressed as nM concentration) are the average (±SE) from 2-4 independent experiments. Boxed number indicates concentration >40 nM. Spike with mutations HV69-70d, Y144d, N501Y, A570D, D614G, P681H (UK) or spike with mutations K417N, E484K, N501Y, D614G (SA-BR). ScFv5 and scFv86 antibodies did not interfere with spike or RBD binding to ACE2 at concentrations ≥40 nM.

bioRxiv preprint doi: https://doi.org/10.1101/2021.06.04.447066; this version posted June 4, 2021. The copyright holder for this preprint (which was not certified by peer review) is the author/funder. All rights reserved. No reuse allowed without permission.

Table 6 Virus neutralization (IC_{50}) of anti-SARS-CoV-2 scFv antibodies in Calu-3 cells

		IC_{50} (nM)	
scFv	**Virus**	**Added to cells 1h after infection**	**Pre-incubated 1h with the virus before cell infection**
76	WT	12.02	<0.1
	D614G	13.02	1.13
	UK	5.23	2.18
76-46	WT	19.35	<0.1
	D614G	21.27	1.53
	UK	ND	ND
76-58	WT	4.56	0.29
	D614G	4.03	0.67
	UK	3.79	1.40
UR	WT	>1400	>1400
	D614G	>1400	>1400
	UK	>1400	>1400
CS*	WT	>1/200	>1/10,000
	D614G	>1/200	>1/10,000
	UK	ND	ND

Serially diluted (3-fold) antibodies were put in contact for 1 h with SARS-CoV-2 WT (Wuhan strain), SARS-CoV-2 variant with D614G mutation or SARS-CoV-2 UK variant, and then added to Calu-3 cell culture, or directly added to the cells 1 h after viral infection. Quantification of viral load was done by RT-qPCR 72 h after infection. IC_{50} values (expressed as nM concentration) were calculated by plotting the inhibition rate against the antibody concentration in GraphPad Prism V8.0 software. UR, scFv unrelated; CS, Covid Serum pool; *Data expressed as dilution giving 50% inhibition.

bioRxiv preprint doi: https://doi.org/10.1101/2021.06.04.447066; this version posted June 4, 2021. The copyright holder for this preprint (which was not certified by peer review) is the author/funder. All rights reserved. No reuse allowed without permission.

References

1. A. Renn, Y. Fu, X. Hu, M. D. Hall, A. Simeonov, Fruitful Neutralizing Antibody Pipeline Brings Hope To Defeat SARS-Cov-2. *Trends Pharmacol. Sci.* **41**, 815-829 (2020). https://doi.org/10.1016/j.tips.2020.07.004.
2. W. S. Lee, A. K. Wheatley, S. J. Kent, B. J. DeKosky, Antibody-dependent enhancement and SARS-CoV-2 vaccines and therapies. *Nat. Microbiol.* **5**, 1185-1191 (2020). https://doi.org/10.1038/s41564-020-00789-5.
3. U.S. Food & Drug Administration, (FDA), "Coronavirus (COVID-19) update: FDA authorizes monoclonal antibodies for treatment of COVID-19" (FDA, 2020, https://www.fda.gov/news-events/press-announcements/coronavirus-covid-19-update-fda-authorizes-monoclonal-antibodies-treatment-covid-19).
4. J. S. Huston, D. Levinson, M. Mudgett-Hunter, M. S. Tai, J. Novotny, M. N. Margolies, R. J. Ridge, R. E. Bruccoleri, E. Haber, R. Crea, Protein engineering of antibody binding sites: recovery of specific activity in an anti-digoxin single-chain Fv analogue produced in Escherichia coli. *Proc. Natl. Acad. Sci. U.S.A.* **85**, 5879-5883 (1988). https://doi.org/10.1073/pnas.85.16.5879.
5. A. Markham, Brolucizumab: First Approval. *Drugs* **79**, 1997–2000 (2019). https://doi.org/10.1007/s40265-019-01231-9.
6. A. C. Walls, Y. J. Park, M. A. Tortorici, A. Wall, A. T. McGuire, D. Veesler, Structure, Function, and Antigenicity of the SARS-CoV-2 Spike Glycoprotein. *Cell* **181**, 281-292.e6 (2020). https://doi.org/10.1016/j.cell.2020.02.058.
7. S. Santopolo, A. Riccio, M. G. Santoro, The biogenesis of SARS-CoV-2 spike glycoprotein: multiple targets for host-directed antiviral therapy. *Biochem. Biophys. Res. Commun.* **538**, 80-87, (2021). https://doi.org/10.1016/j.bbrc.2020.10.080.
8. A. C. Papageorgiou, I. Mohsin, The SARS-CoV-2 Spike Glycoprotein as a Drug and Vaccine Target: Structural Insights into Its Complexes with ACE2 and Antibodies. *Cells* **9**, 2343 (2020). https://doi.org/10.3390/cells9112343.
9. R. Bussani, E. Schneider, L. Zentilin, C. Collesi, H. Ali, L. Braga, M.C. Volpe, A. Colliva, F. Zanconati, G. Berlot, F. Silvestri, S. Zacchigna, M. Giacca, Persistence of viral RNA, pneumocyte syncytia and thrombosis are hallmarks of advanced COVID-19 pathology. *EBioMedicine*. **61,** 103104 (2020). https://doi.org/10.1016/j.ebiom.2020.103104.
10. C. O. Barnes, A. P. West Jr., K. E. Huey-Tubman, M. A. G. Hoffmann, N. G. Sharaf, P. R. Hoffmann, N. Koranda, H. B. Gristick, C. Gaebler, F. Muecksch, J. C. Cetrulo Lorenzi, S. Finkin, T. Hägglöf, A. Hurley, K. G. Millard, Y. Weisblum, F. Schmidt, T. Hatziioannou, P. D. Bieniasz, M. Caskey, D. F. Robbiani, M. C. Nussenzweig, P. J. Bjorkman, Structures of Human Antibodies Bound to SARS-CoV-2 Spike Reveal Common Epitopes and Recurrent Features of Antibodies. *Cell* **182**, 828-842 (2020). https://doi.org/10.1016/j.cell.2020.06.025.
11. J. Huo, A. Le Bas, R. R. Ruza, H. M. E. Duyvestey, H. Mikolajek, T. Malinauskas, T. Kit Tan, P. Rijal, M. Dumoux, P. N. Ward, J. Ren, D. Zhou, P. J. Harrison, M. Weckener, D. K. Clare, V. K. Vogirala, J. Radecke, L. Moynié, Y. Zhao, J. Gilbert-Jaramillo, M. L. Knight, J. A. Tree, K. R. Buttigieg, N. Coombes, M. J. Elmore, M. W. Carroll, L. Carrique, P. N. M. Shah, W. James, A. R. Townsend, D. I. Stuart, R. J. Owens, J. H. Naismith, Neutralizing nanobodies bind SARS-CoV-2 spike RBD and block interaction with ACE2. *Nat. Struct. Mol. Biol.* **27**, 846-854 (2020). https://doi.org/10.1038/s41594-020-0469-6.
12. A. D. Griffiths, M. Malmqvist, J. D. Marks, J. M. Bye, M. J. Embleton, J. McCafferty, M. Baier, K. P. Holliger, B. D. Gorick, N.C. Hughes-Jones, Human anti-self antibodies with high

bioRxiv preprint doi: https://doi.org/10.1101/2021.06.04.447066; this version posted June 4, 2021. The copyright holder for this preprint (which was not certified by peer review) is the author/funder. All rights reserved. No reuse allowed without permission.

specificity from phage display libraries. *EMBO J.* **12**, 725-734 (1993). https://doi.org/10.1002/j.1460-2075.1993.tb05706.x.

13. A. A. Kortt, R. L. Malby, B. Caldwell, L. C. Gruen, N. Ivancic, M. C. Lawrence, G. J. Howlett, R. G. Webster, P. J. Hudson, P. M. Colman, Recombinant anti-sialidase single-chain variable fragment antibody. Characterization, formation of dimer and higher-molecular-mass multimers and the solution of the crystal structure of the single-chain variable fragment/sialidase complex. *Eur. J. Biochem.* **221**, 151-157 (1994). https://doi.org/10.1111/j.1432-1033.1994.tb18724.x.
14. A. Micsonai, F. Wien, L. Kernya, Y. H. Lee, Y. Goto, M. Réfrégiers, J. Kardos, Accurate secondary structure prediction and fold recognition for circular dichroism spectroscopy. *Proc. Natl. Acad. Sci. U. S. A.* **112**, E3095-E3103 (2015). https://doi.org/10.1073/pnas.1500851112.
15. Y. Wu, C. Li, S. Xia, X. Tian, Y. Kong, Z. Wang, C. Gu, R. Zhang, C. Tu, Y. Xie, Z. Yang, L. Lu, S. Jiang, T. Ying, Identification of Human Single-Domain Antibodies against SARS-CoV-2. *Cell Host Microbe* **27**, 891–898 (2020). https://doi.org/10.1016/j.chom.2020.04.023.
16. D. Wiswell, D. Neupane, M. Chen, E. P. Bowman, D. Linn, A. Sawant, A. Chackerian, S. Zhang, E. Escandón, A capillary electrophoresis based approach for the identification of anti-drug antibodies against camelid VHH biologics (Nanobodies®). *J. Pharmacol. Toxicol. Methods* **103**, 106872-106880 (2020). https://doi.org/10.1016/j.vascn.2020.106872.
17. P. Wang, M. S. Nair, L. Liu, S. Iketani, Y. Luo, Y. Guo, M. Wang, J. Yu, B. Zhang, P. D. Kwong, B. S. Graham, J. R. Mascola, J. Y. Chang, M. T. Yin, M. Sobieszczyk, C. A. Kyratsous, L. Shapiro, Z. Sheng, Y. Huang, D. D. Ho, Antibody resistance of SARS-CoV-2 variants B.1.351 and B.1.1.7. *Nature* **593,** 130–135 (2021). https://doi.org/10.1038/s41586-021-03398-2.
18. G. Dudas, S. L. Hong, B. Potter, S. Calvignac-Spencer, F. S. Niatou-Singa, T. B. Tombolomako, T. Fuh-Neba, U. Vickos, M. Ulrich, F. H. Leendertz, K. Khan, A. Watts, I. Olendraitė, J. Snijder, K. N. Wijnant, A. M. J. J. Bonvin, P. Martres, S. Behillil, A. Ayouba, M. Foudi Maidadi, D. Meta Djomsi, C. Godwe, C. Butel, A. Šimaitis, M. Gabrielaitė, M. Katėnaitė, R. Norvilas, L. Raugaitė, R. Jonikas, I. Nasvytienė, Ž. Žemeckienė, D. Gečys, K. Tamušauskaitė, M. Norkienė, E. Vasiliūnaitė, D. Žiogienė, A. Timinskas, M. Šukys, M. Šarauskas, G. Alzbutas, D. Juozapaitė, D. Naumovas, A. Pautienius, A. Vitkauskienė, R. Ugenskienė, A. Gedvilaitė, D. Čereškevičius, V. Lesauskaitė, L. Žemaitis, L. Griškevičius, G. Baele, Travel-driven emergence and spread of SARS-CoV-2 lineage B.1.620 with multiple VOC-like mutations and deletions in Europe. *medRχiv* 2021.05.04.21256637 [Preprint] (2021). https://doi.org/10.1101/2021.05.04.21256637.
19. C. O. Barnes, C. A. Jette, M. E. Abernathy, K. A. Dam, S. R. Esswein, H. B. Gristick, A. G. Malyutin, N. G. Sharaf, K. E. Huey-Tubman, Y. E. Lee, D. F. Robbiani, M. C. Nussenzweig, A. P. West Jr., P. J. Bjorkman, Structural classification of neutralizing antibodies against the SARS-CoV-2 spike receptor-binding domain suggests vaccine and therapeutic strategies. *bioRχiv* 2020.08.30.273920 [Preprint] (2020). https://doi.org/10.1101/2020.08.30.273920.
20. S. Xia, M. Liu, C. Wang, W. Xu, Q. Lan, S. Feng, F. Qi, L. Bao, L. Du, S. Liu, C. Qin, F. Sun, Z. Shi, Y. Zhu, S. Jiang, L. Lu, Inhibition of SARS-CoV-2 (previously 2019-nCoV) infection by a highly potent pan-coronavirus fusion inhibitor targeting its spike protein that harbors a high capacity to mediate membrane fusion. *Cell Res.* **30,** 343–355 (2020). https://doi.org/10.1038/s41422-020-0305-x.
21. D. Zhou, J. F. Chan, B. Zhou, R. Zhou, S. Li, S. Shan, L. Liu, A. J. Zhang, S. J. Chen, Chris C. S. Chan, H. Xu, V. K. M. Poon, S. Yuan, C. Li, K. K. H. Chik, C. C. Y. Chan, J. Cao, C.Y.

bioRxiv preprint doi: https://doi.org/10.1101/2021.06.04.447066; this version posted June 4, 2021. The copyright holder for this preprint (which was not certified by peer review) is the author/funder. All rights reserved. No reuse allowed without permission.

Chan, K. Y. Kwan, Z. Du, T. T. K. Lau, Q. Zhang, J. Zhou, K. K. W. To, L. Zhang, D. D. Ho, K. Y. Yuen, Z. Chen, Robust SARS-CoV-2 infection in nasal turbinates after treatment with systemic neutralizing antibodies. *Cell Host Microbe* **4**, 551-563.e5 (2021). https://doi.org/10.1016/j.chom.2021.02.019.

22. E. Pavoni, G. Monteriù, D. Santapaola, F. Petronzelli, A. M. Anastasi, A. Pelliccia, V. D'Alessio, R. De Santis, O. Minenkova, Tumor-infiltrating B lymphocytes as an efficient source of highly specific immunoglobulins recognizing tumor cells. *BMC Biotechnol.* **7**, 70-86 (2007). https://doi.org/10.1186/1472-6750-7-70.
23. E. Pavoni, O. Minenkova, Vector for efficient selection and/or maturation of an antibody and uses thereof. WO 2007/074496 PCT/IT2006/000876
24. E. Pavoni, G. Monteriù, M. Cianfriglia, O. Minenkova, New display vector reduces biological bias for expression of antibodies in E. coli. *Gene* **391**, 120-129 (2007). https://doi.org/10.1016/j.gene.2006.12.009.
25. M.A. Ramakrishnan, Determination of 50% endpoint titer using a simple formula. *World J. Virol.* **5**, 85-86 (2016). https://doi.org/10.5501/wjv.v5.i2.85.
26. A. Riccio, S. Santopolo, A. Rossi, S. Piacentini, J. F. Rossignol, M. G. Santoro, Impairment of SARS-CoV-2 spike glycoprotein maturation and fusion activity by the broad-spectrum anti-infective drug nitazoxanide. *bioRχiv* 2021.04.12.439201 [Preprint] (20121). https://doi.org/10.1101/2021.04.12.439201.
27. L. Zhang, C. B. Jackson, H Mou, A. Ojha, H. Peng, B. D. Quinlan, E. S. Rangarajan, A. Pan, A. Vanderheiden, M. S. Suthar, W. Li, T. Izard, C. Rader, M. Farzan, H. Choe, SARS-CoV-2 spike-protein D614G mutation increases virion spike density and infectivity. *Nat. Commun.* **11**, 6013-6021 (2020). https://doi.org/10.1038/s41467-020-19808-4.
28. X. Ou, Y. Liu, X. Lei, P. Li, D. Mi, L. Ren, L. Guo, R. Guo, T. Chen, J. Hu, Z. Xiang, Z. Mu, X. Chen, J. Chen, K. Hu, Q. Jin, J. Wang, Z. Qian, Characterization of spike glycoprotein of SARSCoV-2 on virus entry and its immune cross-reactivity with SARS-CoV. *Nat. Commun.* **11**, 1620-1631 (2020). https://doi.org/10.1038/s41467-020-15562-9.
29. J. Buchrieser, J. Dufloo, M. Hubert, B. Monel, D. Planas, Maaran Michael Rajah, C. Planchais, F. Porrot, F. G. Benhassine, S. Van der Werf, N. Casartelli, H. Mouquet, T. Bruel, O. Schwartz, Syncytia formation by SARS-CoV-2-infected cells. *EMBO J.* **39**, e106267, (2020). https://doi.org/10.15252/embj.2020106267.
30. E. Campeau, V. E. Ruhl, F. Rodier, C. L. Smith, B. L. Rahmberg, J. O. Fuss, J. Campisi, P. Yaswen, P. K. Cooper, P. D. Kaufman, A versatile viral system for expression and depletion of proteins in mammalian cells. *PLoS One* **4**, e6529 (2009). https://doi.org/10.1371/journal.pone.0006529.
31. E. Davidson, B. J. Doranz, A high-throughput shotgun mutagenesis approach to mapping B-cell antibody epitope. *Immunology* **143**, 13-20 (2014). https://doi.org/10.1111/imm.12323.
32. T. Maniatis, E. F. Fritsch, J. Sambrook, Ed., Molecular Cloning: A Laboratory *Manual* (Cold Spring Harbor, New York, 1982).

Supplementary Materials

Materials and Methods

Supplementary Tables 1, 2

Supplementary Figures 1-8

bioRxiv preprint doi: https://doi.org/10.1101/2021.06.04.447066; this version posted June 4, 2021. The copyright holder for this preprint (which was not certified by peer review) is the author/funder. All rights reserved. No reuse allowed without permission.

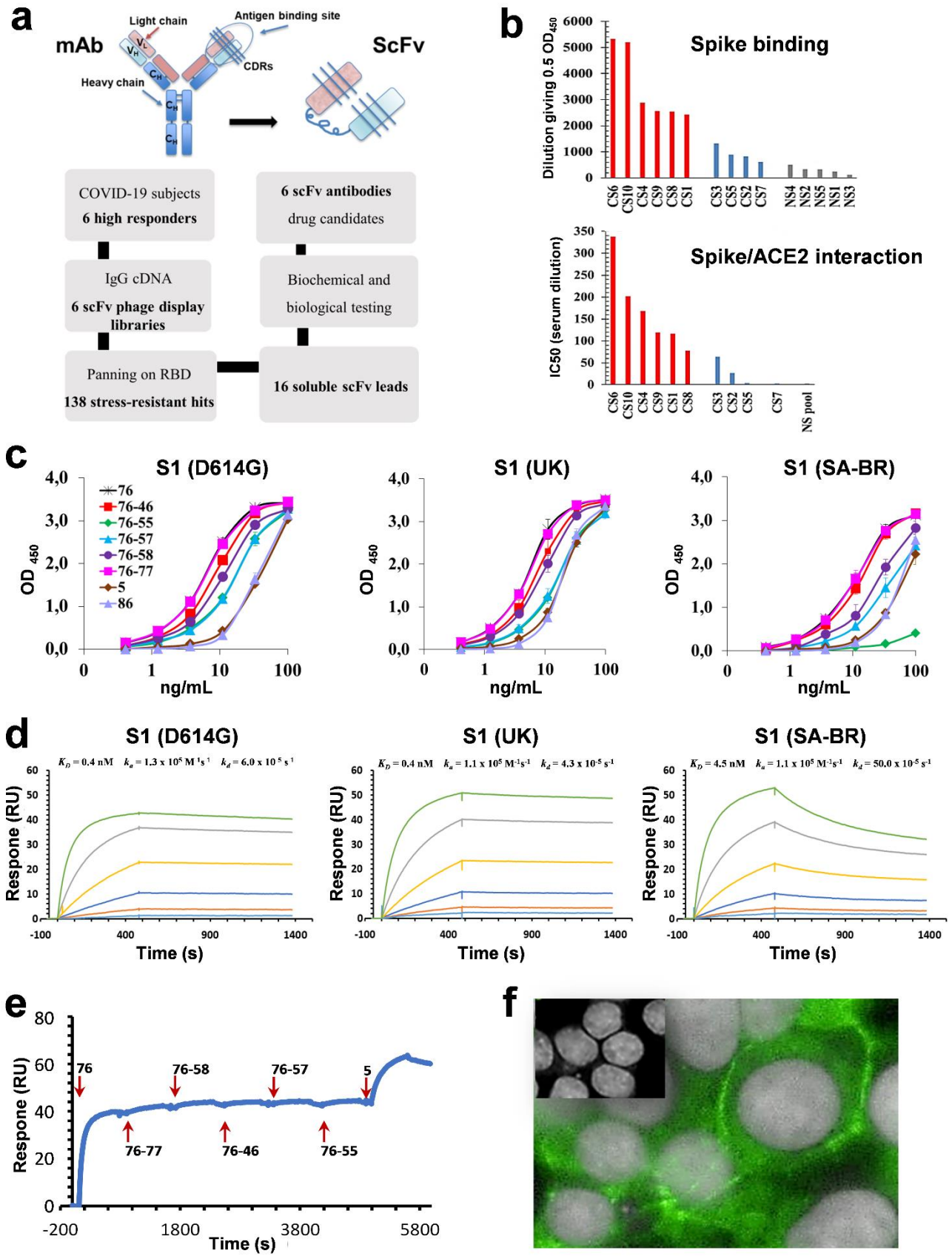

Figure 1

bioRxiv preprint doi: https://doi.org/10.1101/2021.06.04.447066; this version posted June 4, 2021. The copyright holder for this preprint (which was not certified by peer review) is the author/funder. All rights reserved. No reuse allowed without permission.

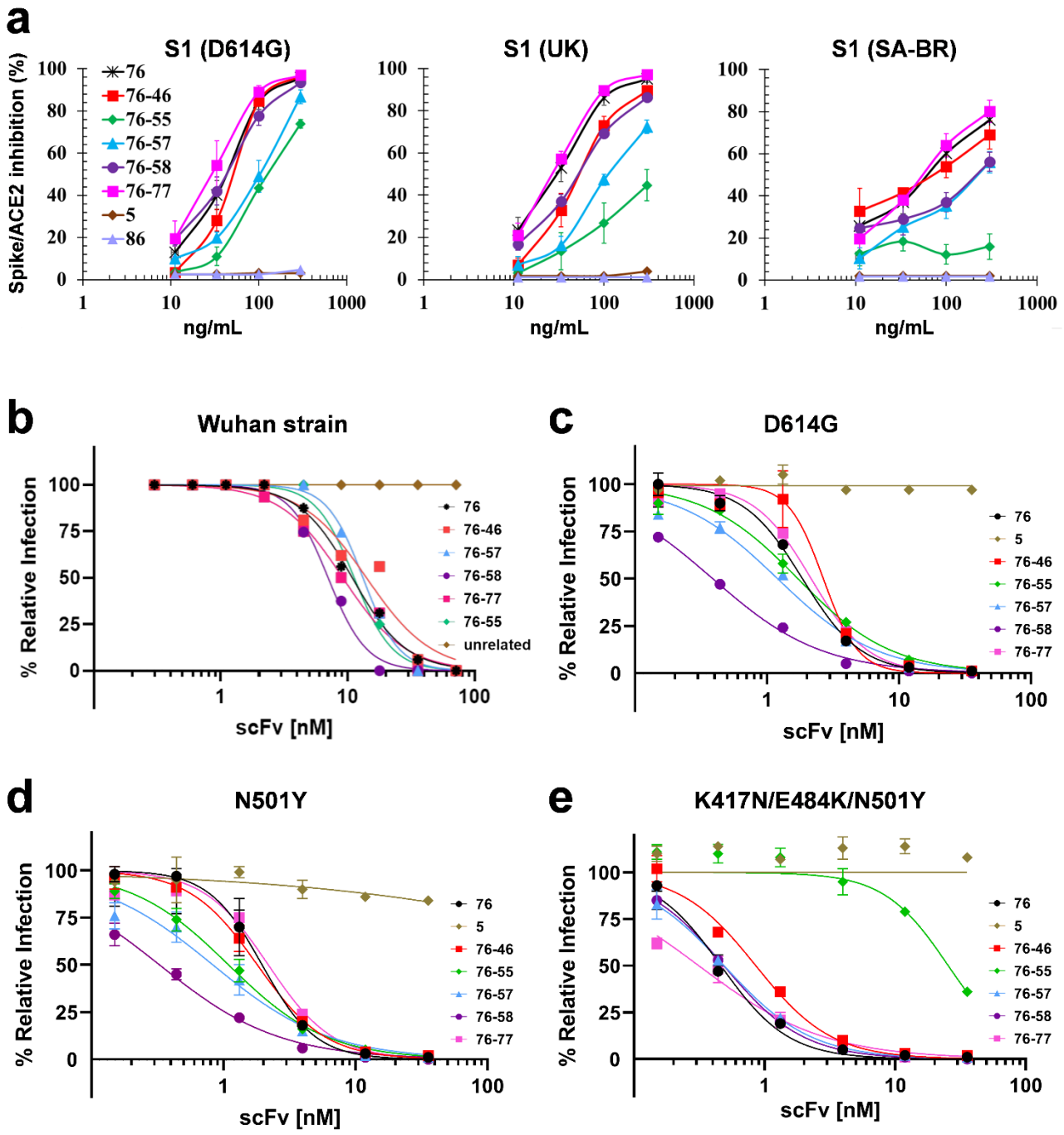

Figure 2

bioRxiv preprint doi: https://doi.org/10.1101/2021.06.04.447066; this version posted June 4, 2021. The copyright holder for this preprint (which was not certified by peer review) is the author/funder. All rights reserved. No reuse allowed without permission.

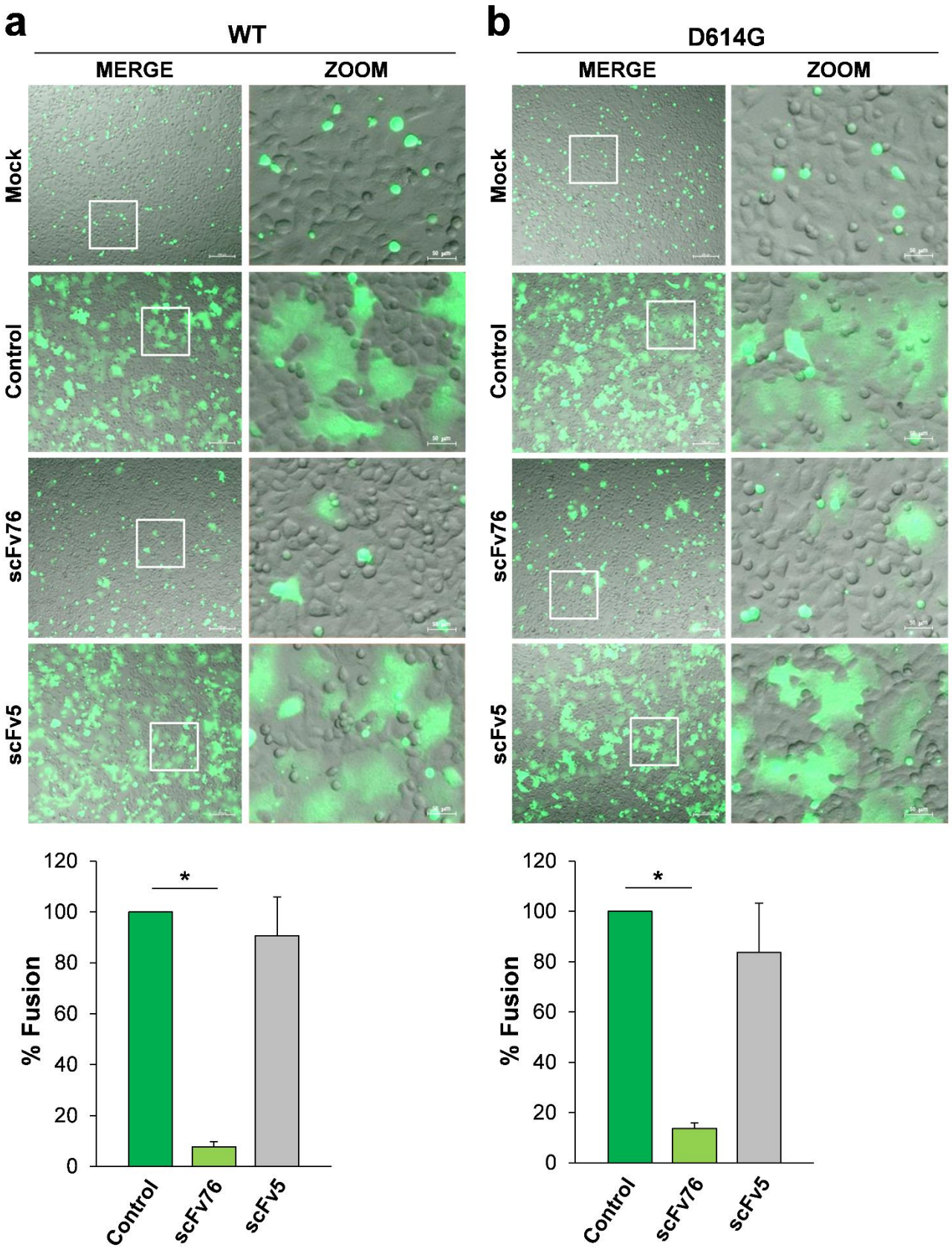

Figure 3

bioRxiv preprint doi: https://doi.org/10.1101/2021.06.04.447066; this version posted June 4, 2021. The copyright holder for this preprint (which was not certified by peer review) is the author/funder. All rights reserved. No reuse allowed without permission.

a

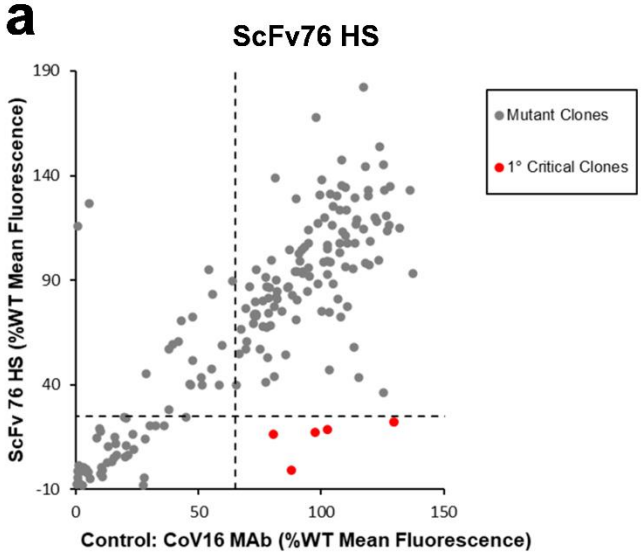

b

Binding Reactivity (%WT)		
Mutation	**ScFv 76 HS**	**CoV16 MAb**
L455A	22 (10)	129.7 (4)
F456A	-0.8 (0)	88 (22)
Y473A	16.4 (3)	80.5 (1)
N487A	17.3 (12)	97.3 (7)
Y489A	18.5 (4)	102.6 (17)

c

d

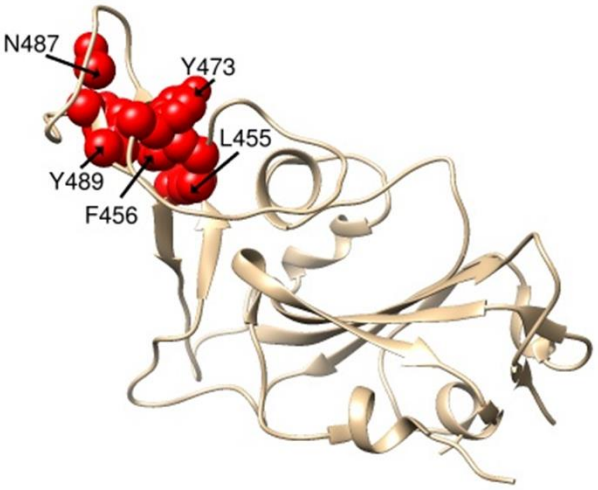

Figure 4

bioRxiv preprint doi: https://doi.org/10.1101/2021.06.04.447066; this version posted June 4, 2021. The copyright holder for this preprint (which was not certified by peer review) is the author/funder. All rights reserved. No reuse allowed without permission.

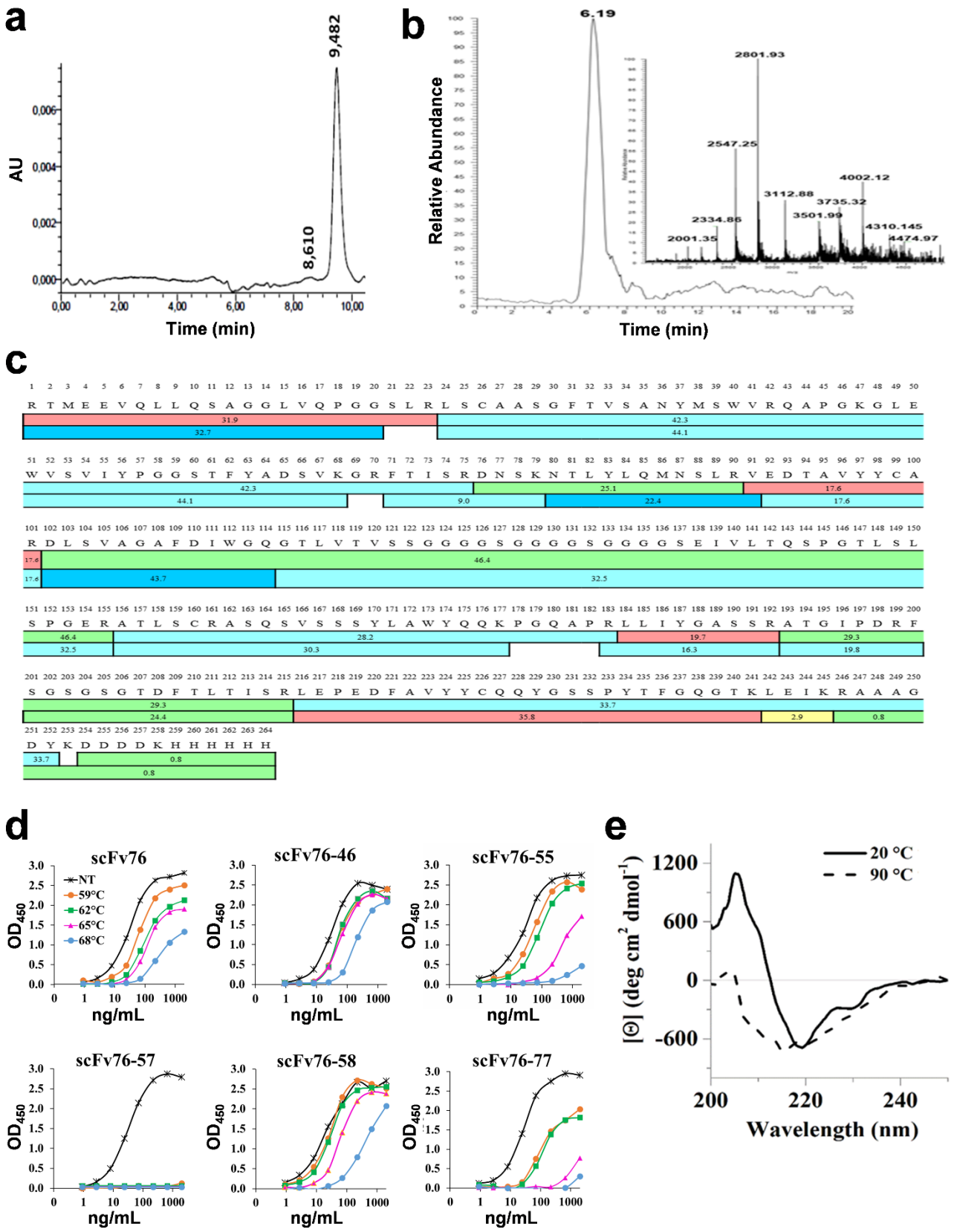

Figure 5

bioRxiv preprint doi: https://doi.org/10.1101/2021.06.04.447066; this version posted June 4, 2021. The copyright holder for this preprint (which was not certified by peer review) is the author/funder. All rights reserved. No reuse allowed without permission.

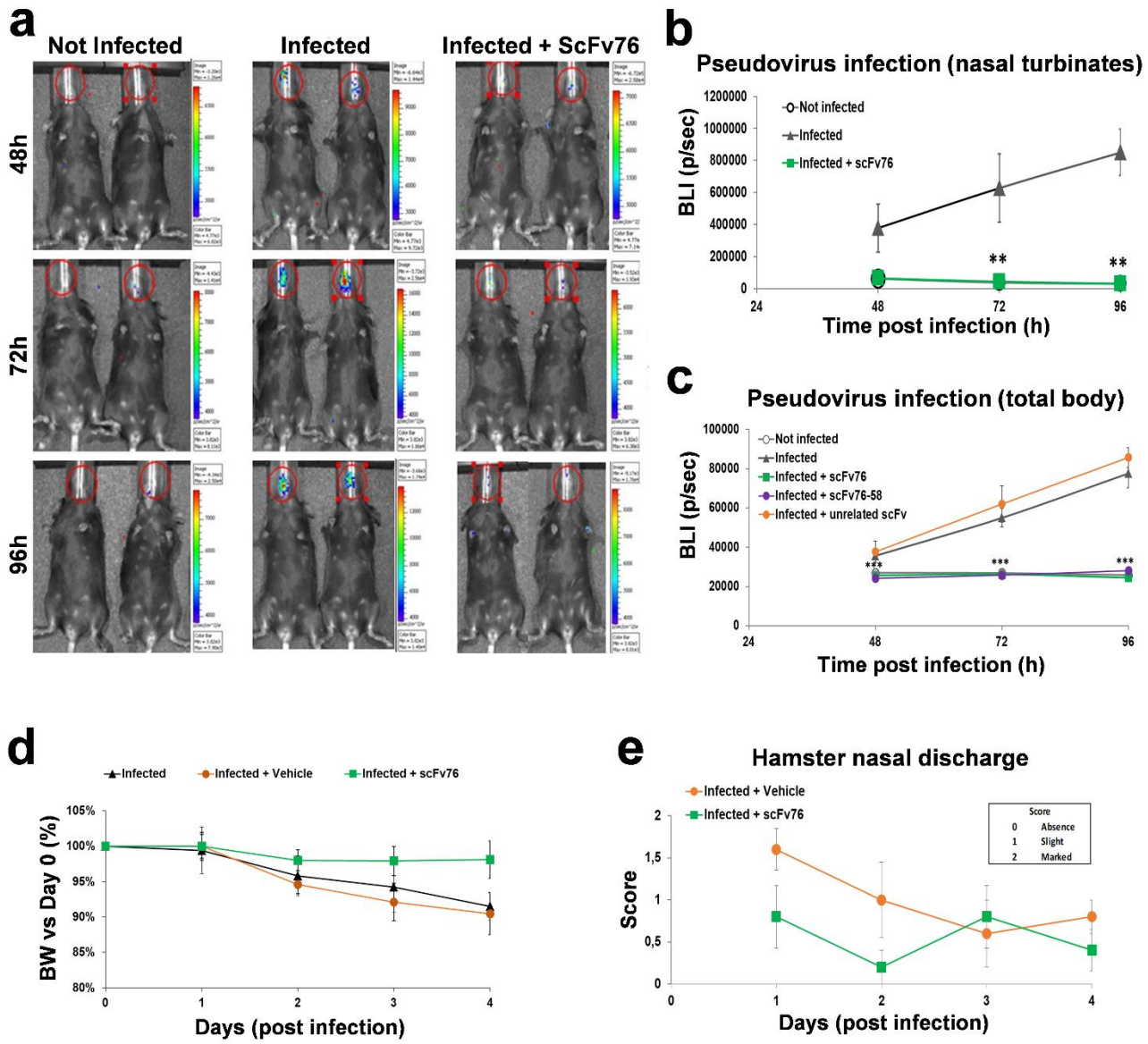

Figure 6